8-14-2012

Syntheses of Boron Nitride Nanotubes from Borazine and Decaborane Molecular Precursors by Catalytic Chemical Vapor Deposition with a Floating Nickel Catalyst

Shahana Chatterjee
University of Pennsylvania,

Myung Jong Kim
USAF; University of Pennsylvania; Korea Institute of Science & Technology

Dmitri Zakharov
Purdue University, Birck Nanotechnology Center, zakharov@purdue.edu

Seung Min Kim
Purdue University, Birck Nanotechnology Center

Eric A. Stach
Purdue University, Birck Nanotechnology Center, Stach.Purdue@gmail.com

See next page for additional authors

CHEMISTRY OF MATERIALS

Article

pubs.acs.org/cm

Syntheses of Boron Nitride Nanotubes from Borazine and Decaborane Molecular Precursors by Catalytic Chemical Vapor Deposition with a Floating Nickel Catalyst

Shahana Chatterjee,[†] Myung Jong Kim,[†,‡,§] Dmitri N. Zakharov,[∥] Seung Min Kim,[∥,⊥] Eric A. Stach,[∥,⊗] Benji Maruyama,*[,‡] and Larry G. Sneddon*[,†]

[†]Department of Chemistry, University of Pennsylvania, Philadelphia, Pennsylvania 19104-6323, United States

[‡]Materials and Manufacturing Directorate, Air Force Research Laboratory, Wright Patterson Air Force Base, Ohio 45433, United States

[§]Institute of Advanced Composite Materials, Korea Institute of Science and Technology, Dunsan-ri 864-9, Bondong-eup, Wanju-gun, Jeollabuk-do, Republic of Korea

[∥]School of Materials Engineering and Birck Nanotechnology Center, Purdue University, 1205 West State Street, West Lafayette, Indiana 47907, United States

Supporting Information

ABSTRACT: Multi- and double-walled boron nitride nanotubes (BNNTs) have been synthesized with the aid of a floating nickel catalyst via the catalytic chemical vapor deposition (CCVD) of either the amine-borane borazine ($B_3N_3H_6$) or the polyhedral-borane decaborane ($B_{10}H_{14}$) molecular precursors in ammonia atmospheres. Both sets of BNNTs were crystalline with highly ordered structures. The BNNTs grown at 1200 °C from borazine were mainly double-walled, with lengths up to 0.2 μm and ∼2 nm diameters. The BNNTs grown at 1200−1300 °C from decaborane were double- and multiwalled, with the double-walled nanotubes having ∼2 nm inner diameters and the multiwalled nanotubes (∼10 walls) having ∼4−5 nm inner diameters and ∼12−14 nm outer diameters. BNNTs grown from decaborane at 1300 °C were longer, averaging ∼0.6 μm, whereas those grown at 1200 °C had average lengths of ∼0.2 μm. The BNNTs were characterized using scanning and transmission electron microscopies (SEM and TEM), and electron energy loss spectroscopy (EELS). The floating catalyst method provides a catalytic and potentially scalable route to BNNTs with low defect density from safe and commercially available precursor compounds.

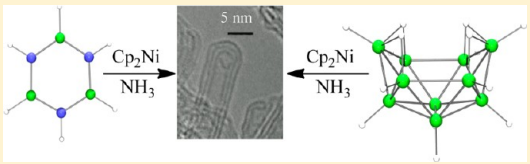

KEYWORDS: *boron nitride nanotubes, chemical vapor deposition, nickel, borazine, decaborane, floating catalyst*

INTRODUCTION

Owing to their remarkable electronic, mechanical, and optical properties, carbon nanotubes (CNTs) have been an extensively studied one-dimensional (1-D) nanostructure.[1−3] Boron nitride nanotubes (BNNTs) are isostructural and isoelectronic with CNTs, where alternating sp^2-hybridized boron and nitrogen atoms replace the carbons in the hexagonal lattice structure. This elemental substitution results in a number of important property changes including an increased chemical inertness and oxidation resistance up to 800 °C,[4] as well as a large band gap (∼5 eV)[5−9] that is independent of tube parameters and which can be tuned by a giant Stark effect.[10,11] However, BNNTs retain both the mechanical strength[12] and thermal conductivity[13−15] of CNTs. This combination of properties makes BNNTs attractive for potential applications in nano- and optoelectronics, nanocomposites, hydrogen storage devices, and as chemical sensors.[16−20] As a result, there has been great recent interest in the development BNNT synthetic methods.

Following the discovery of hollow tubular forms of BN by Hamilton et al.[21] and single- and multiwalled BNNTs by Loiseau et al.[22] and Chopra et al.,[23] respectively, methods analogous to those previously used for CNT syntheses have been explored as routes to BNNTs. Hexagonal boron nitride and metal borides were initially used as the boron source and early work showed that both arc discharge[22−29] and laser ablation[30−35] methods in nitrogen atmospheres could be used to produce highly crystalline BNNTs with small diameters and lengths up to hundreds of micrometers. However, the high operational temperatures of these processes (∼3000−4000 °C) have limited their scales.

BNNT syntheses employing elemental boron have included ball-milling boron powder under ammonia followed by high temperature annealing under ammonia or nitrogen in the absence[36−39] or presence[40,41] of additional catalysts, and thermal chemical vapor deposition (CVD) reactions of boron powder and ammonia in the presence of metal oxide catalysts, including Fe_2O_3,[42−44] Ga_2O_3,[45,46] MgO,[47−50] and Li_2O,[51] or metallic-iron[52] and nickel-boride[53] catalysts. A pressurized

Received: February 24, 2012
Revised: June 1, 2012
Published: July 23, 2012

   dx.doi.org/10.1021/cm3006088 | *Chem. Mater.* 2012, 24, 2872−2879

vapor condensation method[54] where boron vapors at temperatures over 4000 °C were allowed to condense at elevated nitrogen pressures has also recently been reported to yield long fibrils of BNNTs.

More recent BNNT syntheses have used the pyrolysis of chemical precursors, including B−N−O[55,56] and B−N−Si[57] polymers or mixtures of ammonia-borane with ferrocene[58] in nitrogen, iron borate[59] with Mg[60] or Mg/Co[61] in ammonia, and boric oxide with polypropylene and carbon black[62] in ammonia. BNNTs have also been synthesized by thermal CVD from borazine using Co, Ni, or nickel-boride catalysts at 1000−1100 °C[63] and by the plasma-enhanced CVD (PECVD) of a diborane (B_2H_6) ammonia-hydrogen mixture on iron-, nickel-, or cobalt-coated silicon wafers.[64−67] BNNTs synthesized by these methods generally had large diameters and were often not highly crystalline and defect free.

Until our recent work,[68] one CNT synthesis route that had not been explored for BNNTs was the "floating catalyst" method. This catalytic chemical vapor deposition (CCVD) method employs precursor compounds, which in the case of CNTs has included benzene or acetylene, to react with Fe, Co, or Ni nanoparticles (NPs), the "floating catalysts", that are generated in situ in the gas phase.[69−79] We have communicated some initial studies demonstrating that this method could be used to synthesize BNNTs by the reaction of borazine in an ammonia atmosphere catalyzed by Ni NPs generated in situ from nickelocene, $(\eta^5\text{-}C_5H_5)_2Ni$.[68] In this paper, we report the extension of this floating catalyst process for BNNT synthesis to include the first use of the commercially available polyborane decaborane, $B_{10}H_{14}$, as a safe and alternative BNNT precursor.

RESULTS AND DISCUSSION

Metal-catalyzed nanotube syntheses are based on the assumption that NTs grow by a diffusion mechanism analogous to the macroscopic vapor−liquid−solid (VLS) mechanism found for the growth of silicon whiskers, carbon filaments, or metallic nanowires.[1,80−82] For CNTs, the growth is facilitated by carbon solubility in the liquid metal particles at the CNT growth temperatures.[3,83] The higher solubility of boron in Ni compared to other transition metals[84] led us to select Ni as the catalyst for our BNNT syntheses. The organometallic sandwich complex nickelocene was employed as the Ni NP precursor, since it has been shown to be an excellent source of metallic Ni under reducing conditions. Floating Ni NP catalysts derived from nickelocene had also already been used to generate both single-walled and multiwalled CNTs from acetylene, benzene, and thiophene precursors in hydrogen and argon atmospheres at 900−1100 °C.[69−71,75] Nickelocene has the advantages that it is kinetically and thermodynamically stable in inert atmospheres up to 300 °C and can be sublimed with an easily temperature-regulated vapor pressure.[85,86]

A potential boron-containing chemical precursor for the CCVD synthesis of BNNTs would ideally be (1) safe and easy to handle, (2) commercially available, and (3) sufficiently stable to avoid the formation of unwanted side products at high temperatures that could increase defects and decrease BNNT yields. In our studies, we compared the reactivities and advantages of two different types of molecular precursors, borazine and decaborane. The amine-borane borazine[87,88] is a "single-source" precursor already having both the ideal 1:1 B:N composition and the preformed hexagonal ring structure of h-BN with sp^2-hybridized boron and nitrogen atoms. Early surface science studies demonstrated that borazine can be used to grow h-BN monolayers on many single-crystal metals.[89−94] Borazine has the advantage that it is a volatile liquid with sufficient vapor pressure to be easily carried into the growth zone by an inert carrier gas; however, it is also air and moisture sensitive and will fragment and polymerize as low as 70 °C to generate undesirable side products that could reduce the overall yield of BNNTs.[95,96] In contrast, the polyhedral-borane decaborane[97] is an air and moisture stable crystalline solid that does not decompose up to ∼300 °C under inert conditions. It also has an easily temperature-controlled vapor pressure over the room temperature to 100 °C range that allows it to be readily sublimed without decomposition into the gas phase and then transported into the reaction zone of a CVD furnace by an inert carrier gas.[98] But, since it does not contain nitrogen, decaborane must be additionally reacted in the growth zone with a nitrogen source, such as ammonia, to form BNNTs. Nevertheless, we have recently demonstrated that such decaborane/ammonia reactions can provide efficient routes to BN nanosheets on metallic substrates.[99]

The experimental setups for BNNT syntheses from borazine and decaborane are shown in the Supporting Information, Figures S1 and S2, and the details of the representative reactions are given in Tables 1−3. With both borazine and decaborane, the nickelocene precatalyst was vaporized and carried into the reaction zone by heating a vessel containing solid nickelocene under a flow of ammonia, nitrogen, or hydrogen to the desired vaporization temperature (∼80−100 °C). For reactions with borazine, a bubbler containing liquid borazine was maintained under a nitrogen flow at the temperature (∼ −20 to 20 °C) of the desired borazine vapor pressure with a cooling bath. For reactions with decaborane, a flow-through vessel containing solid decaborane was heated under a nitrogen flow to the desired vaporization temperature (∼90−100 °C). In both sets of experiments, the relative flow rates of nickelocene to borazine or nickelocene to decaborane were controlled by regulating the vessel temperatures and the carrier gas flow rates. The precursor and nickelocene gas streams were allowed to mix in the growth zone of a Lindberg tube furnace at temperatures between 1000 and 1400 °C. Additional flows of ammonia and/or nitrogen were supplied to the furnace through separate inlets. Over the several-hour course of the reactions, the BN nanomaterials were collected at room temperature on a grid with a glass fiber filter located

Table 1. Summary of BNNT Syntheses with Borazine at 1000−1300 °C

		borazine flow		nickelocene flow		NH_3 flow	
exp.	growth temp. (°C)	bubbler temp. (°C)	carrier rate (sccm)[a]	bubbler temp. (°C)	carrier rate (sccm)	rate (sccm)	growth time (h)
A	1200	20	1	90	350[b]	0	1
B	1200	20	1	90	350[c]	0	0.5
C	1200	−20	10	80	300[c]	0	3
D	1000	−20	3	80	100[c]	0	3
E	1100	−20	3	80	100[c]	0	5
F	1200	−20	3	80	100[c]	0	3
G	1300	−20	3	80	100[c]	0	3
H	1200	−20	3	80	100[d]	100	3

[a]The carrier gas for borazine was UHP nitrogen. [b]The carrier gas for nickelocene was UHP hydrogen. [c]The carrier gas for nickelocene was UHP ammonia. [d]The carrier gas for nickelocene was UHP nitrogen.

dx.doi.org/10.1021/cm3006088 | Chem. Mater. 2012, 24, 2872−2879

downstream in the pyrolysis tube near the exit of the furnace. For the subsequent analyses, the as-grown samples were washed off the collection grid with ethanol. The solution was ultrasonicated and then dropped on a holey carbon TEM grid to enable study by transmission electron microscopy (TEM) at 200 kV and electron energy loss spectroscopy (EELS) at 300 kV. Samples for scanning electron microscopy (SEM) analyses were prepared by depositing the BN nanomaterials on carbon tape on SEM stubs and sputter coating these materials with Au/Pd.

As given in the Experimental Section, systematic variations in the reaction zone temperature, the relative flow rates (F_{pr}), and the mole-fractions (χ_{pr}) of the chemical precursor, the nickelocene catalyst, the ammonia reactant, and the nitrogen carrier were each investigated to determine their effects on BNNT yields and quality. Discussed below and summarized in Tables 1−3 are only those changes that had a significant effect on either the BNNT yields or structures.

No BNNTs were ever found to grow in the absence of the nickelocene precatalyst (control exps. I and II). For decaborane, it was also observed that no tube-like structures could be grown in the absence of ammonia (control exp. III).

The previous CCVD syntheses of CNTs employing floating Ni NPs had typically used hydrogen gas mixed into their feed streams as the nickelocene reducing agent, but as given in the representative experiment (exp. A) in Table 1, no BNNT formation was observed for analogous borazine/nickelocene reactions under hydrogen flows. However, depending upon the borazine pressure and flow rates, when the borazine/nickelocene reactions were carried out using ammonia as the nickelocene reducing agent, either BN nanofibers or BNNTs were produced (Table 1). Thus, only BN nanofibers were observed in 1200 °C reactions that employed nickelocene (~1.4 Torr) and ammonia (350 sccm) with higher vapor pressures of borazine (~166 Torr, 1 sccm nitrogen) (exp. B). Likewise, reactions with lower borazine vapor pressures (~22 Torr), but with high carrier gas flow rates for both borazine (10 sccm nitrogen) and nickelocene (~1.1 Torr, 300 sccm ammonia) (exp. C), also gave only BN nanofibers. These nanofibers (Figure 1) were 500 nm to 1 μm long and had diameters of ~20−30 nm, but appeared to be largely amorphous by TEM.

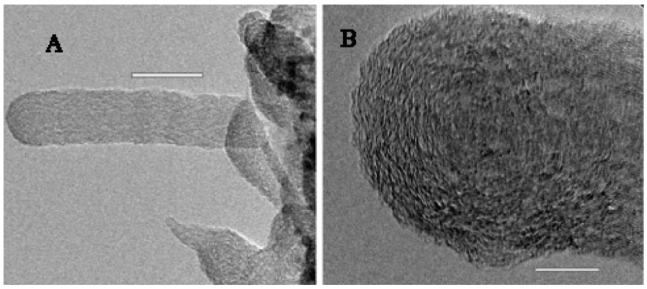

Figure 1. TEM images of BN nanofibers obtained from borazine at 1200 °C. Scale bars: A, 50 nm; B, 10 nm.

The best conditions for producing BNNTs from borazine proved to be 1200 °C reactions that used lower vapor pressures and lower carrier flow rates of both borazine, (~22 Torr, 3 sccm nitrogen) and nickelocene (~1.1 Torr), with ammonia as the carrier gas (100 sccm ammonia) for the nickelocene. Under these conditions, TEM analysis of the products showed crystalline double-walled BNNTs (exp. F) having well-ordered structures with ~2 nm inner diameters and 100−200 nm lengths (Figure 2**B**). In other experiments, BNNTs were

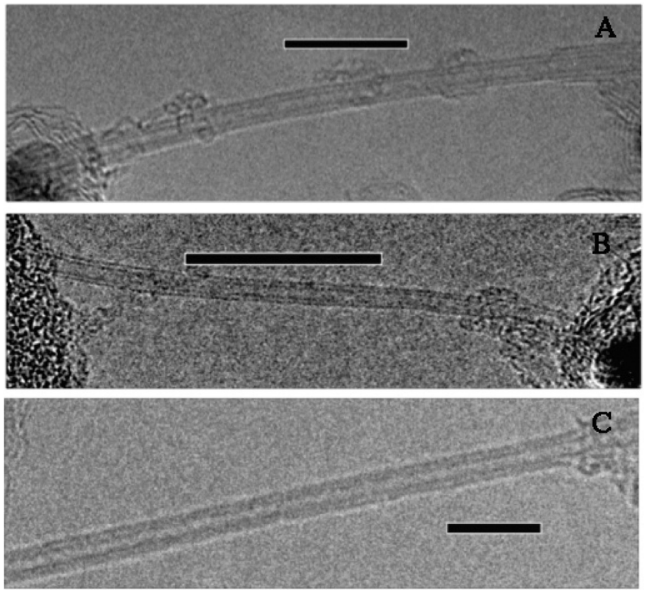

Figure 2. TEM images of BNNTs obtained from borazine at A, 1100 °C; B, 1200 °C; and C, 1300 °C. Scale bars: A, C, 10 nm; B, 20 nm.

observed at temperatures as low as 1100 °C (exp. E, Figure 2**A**), but these tubes were not as uniform as those formed at 1200 and 1300 °C (exp. G) (Figure 2**C**).

The optimum conditions for the decaborane/ammonia reactions (Tables 2 and 3) proved to be 3 h growth at 1200 °C employing nearly equal mole ratios of decaborane and nickelocene (exps. J and K) in the growth zone. As shown in the SEM image in Figure 3**A**, numerous nanodimensional tube-like structures with ~0.1−0.3 μm lengths were obtained under these conditions (Figure 3**B**). TEM analysis showed that most of the BNNTs were few-walled (1−5 walls) with ~2 nm inner diameters (Figures 4**A**−**C**), but that some multiwalled BNNTs (~10−14 walls) with ~4−5 nm inner diameters and ~12−14 nm outer diameters (Figures 4**D**−**E**) were also observed. Other experiments showed that BNNTs, with up to 5 walls and ~2 nm inner diameters (exp. I, Supporting Information, Figure S3), could be produced at temperatures as low as 1100 °C. However, as was the case for borazine, higher temperatures reactions produced longer and more uniform tubes, with the multiwalled BNNTs that were the primary products at 1300 °C (exp. Q) (Figure 5) having ~0.2−0.6 μm lengths. Raising the temperature to 1400 °C (exp. R) gave mostly 1−5 wall BNNTs, averaging ~0.2 μm in length (Supporting Information, Figure S4) and ~2 nm inner diameters, but these tubes exhibited more defects that those grown at 1200 or 1300 °C (Supporting Information, Figure S4).

The TEM analyses of BNNTs from both borazine and decaborane confirmed formation of hollow tube-like structures with crystalline walls that exhibited lattice fringe patterns and ~0.34 nm interwall spacings characteristic of h-BN.[100] As can be seen in the examples in Figures 4 and 5, the BNNTs obtained from both borazine and decaborane had nearly flat closed ends. Such structures are characteristic of BNNTs, since B−N bonds are proposed to be energetically more favored than either B−B or B−N bonds, thus leading to the use of even-

Table 2. Summary of BNNT Syntheses with Decaborane at 1100−1400 °C

		decaborane flow		nickelocene flow		NH_3 flow	N_2 flow	
exp.	growth temp. (°C)	bubbler temp. (°C)	carrier rate (sccm)[a]	bubbler temp. (°C)	carrier rate (sccm)	rate (sccm)	rate (sccm)	growth time (h)
I	1100	90	12	80	100[b]	100	0	1.5
J	1200	90	12	80	100[b]	100	0	3
K	1200	100	5	80	100[b]	100	0	3
L	1200	90	5	80	100[b]	100	0	3
M	1200	100	5	80	100[b]	100	200	3
N	1200	100	5	80	300[b]	100	0	3
O	1300	90	12	98	100[b]	100	0	3
P	1200	100	5	80	100[c]	0	0	3
Q	1300	90	12	80	100[b]	100	0	3
R	1400	90	12	80	100[b]	100	0	2

[a]The carrier gas for decaborane was UHP nitrogen. [b]The carrier gas for nickelocene was UHP nitrogen. [c]The carrier gas for nickelocene was UHP ammonia.

Table 3. Summary of Flow Rate and Mole Fraction Data for the BNNT Syntheses with Decaborane at 1200−1300°C

	flow rate F_{pr} (sccm)		mole fraction $\chi_{pr} \times 10^3$		
exp.	decaborane	nickelocene	decaborane	nickelocene	relative yields of BNNTS
J[a]	0.16	0.14	0.75	0.66	maximum
K[a]	0.13	0.14	0.63	0.68	maximum
L[a]	0.07	0.14	0.34	0.68	low
M[a]	0.13	0.14	0.32	0.34	low
N[a]	0.13	0.43	0.32	1.06	moderate
O[b]	0.16	0.47	0.75	2.21	very low

[a]exp. at 1200 °C. [b]exp at 1300 °C.

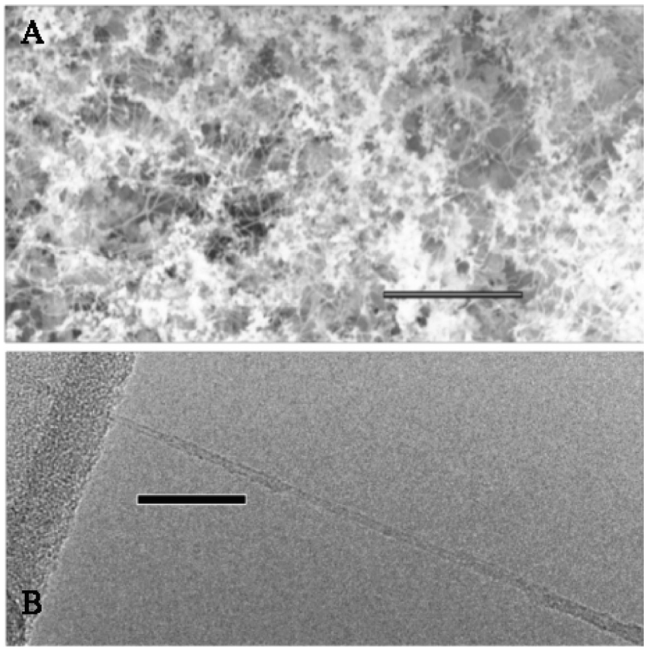

Figure 3. A, SEM and B, TEM images of BNNTs obtained from decaborane at 1200 °C. Scale bars: A, 1 μm; B, 50 nm.

numbered B−N ring structures (such as, squares and octagons instead of pentagons and heptagons) in the tube closure process that produce flat ends.[101,102] Some of the multiwalled BNNTs also exhibited inner shells nested inside outer shells (Figures 4D−E). While the borazine-derived BNNTs were mostly double-walled, multiwalled BNNTs were the primary

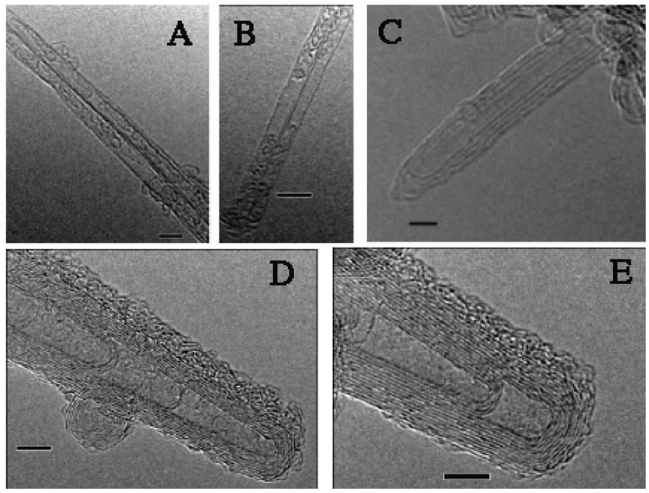

Figure 4. High-resolution TEM images of BNNTs obtained from decaborane at 1200 °C. Scale bars: A, B, D, E, 5 nm; C, 2 nm.

products from decaborane. As noted earlier for CNTs, the carbon content of the precursor can influence the number of nanotube walls.[3] Thus, the higher boron content of decaborane (10 borons per molecule) compared to borazine (3 borons per molecule) should favor the observed multiwall compositions.

The as-grown BN products from the reactions with decaborane also contained hollow ellipsoidal- and spherical-structured BN nanomaterials (Figure 6) that were similar to those that have been reported in other BNNT syntheses.[103−107] The ellipsoidal structures had multiple walls with ∼5 nm inner diameters and lengths up to ∼30 nm (Figure 6A). For the spherical materials, both few-walled structures with large inner diameters (>10 nm) and multiwalled structures with small (∼2 nm) inner diameters were observed (Figure 6**B**-**C**). Hollow BN NPs with layered hexagonal structures and multiple walls, up to ∼40 nm in length, were also found (Figure 6D).

The EELS data from the BNNTs derived from both borazine and decaborane (Figure 7) showed the sharp boron and nitrogen K-edges that are characteristic of sp^2-hybridized boron and nitrogen.[108,109] The spectra from the as-prepared samples also showed very small peaks from amorphous-carbon K edges, most likely from the decomposed nickelocene catalyst. Similar amorphous-carbon peaks were observed by Arenal et al.[34] in single-walled BNNTs grown by laser vaporization and likewise attributed to carbon contamination during the growth process. As shown in Supporting Information, Figure S5, we found that

dx.doi.org/10.1021/cm3006088 | *Chem. Mater.* 2012, 24, 2872−2879

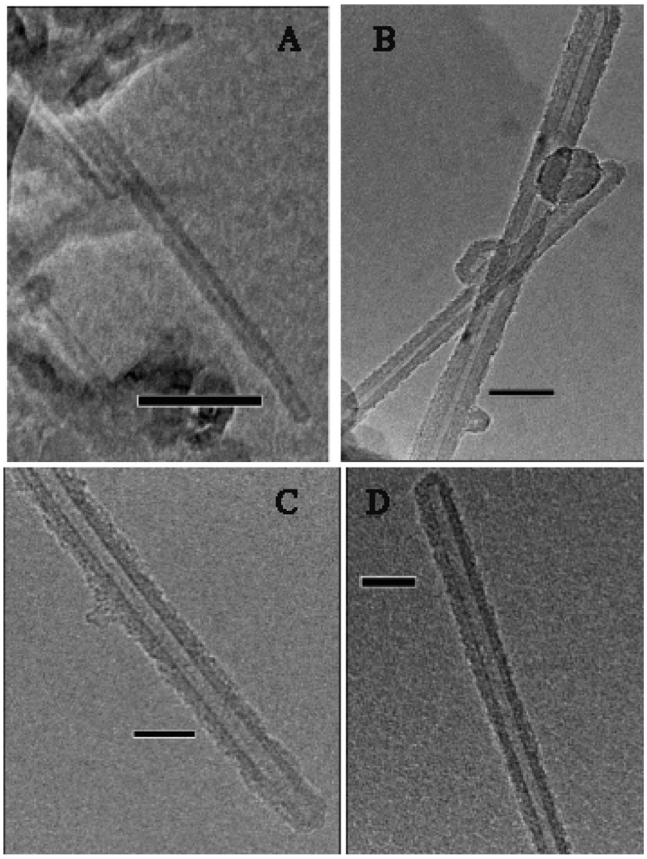

Figure 5. TEM images of BNNTs obtained from decaborane at 1300 °C. Scale bars: A, B, 50 nm; C, D, 20 nm.

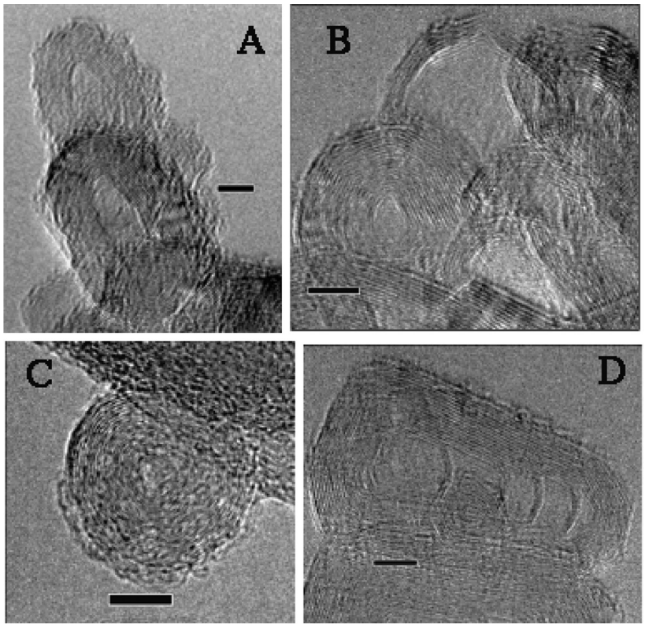

Figure 6. TEM images of polyhedral BN nanostructures obtained at 1200 °C (A), 1300 °C (B, D), and 1400 °C (C) from decaborane. Scale bars: A, B, D, 5 nm; C, 10 nm.

these that these amorphous C peaks could be completely removed from one of the as-generated samples without damaging the BNNT structure by air oxidation at 600 °C,

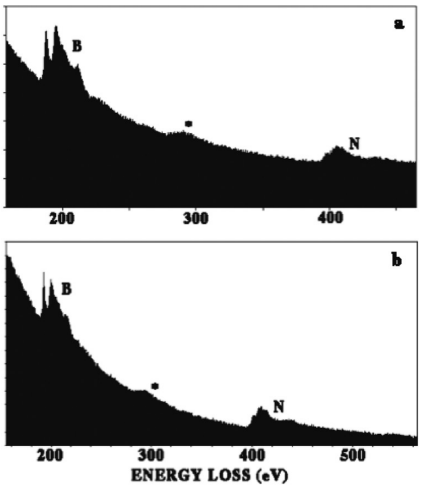

Figure 7. Electron energy loss spectra (EELS) of BNNTs obtained from (a) borazine and (b) decaborane at 1200 °C. Peaks indicated by * are from amorphous carbon.

with the subsequent EELS analysis of the oxidized samples showing only B and N.

The exact mechanisms of BNNT growth in the borazine and decaborane floating-catalyst CCVD reactions are still to be determined. However, borazine and decaborane based compounds are known to react with many metals at high temperatures to form metal boride phases,[110,111] and this reactivity coupled with the fact that nickel boride has previously been shown[53,63] to catalyze BNNT growth suggests a reaction pathway involving the initial formation of nickel boride growth sites on the Ni NPs that can then bind either borazine or decaborane. Borazine is known[95,96] to undergo dehydropolymerization to form B−N linked polyborazylene polymers, $[B_3N_3H_{\sim 4}]_x$, that can then be readily converted to boron nitride at high temperatures. On the basis of these known reactions, a reasonable BNNT growth mechanism from borazine could involve initial borazine binding to the catalyst active sites, followed by further borazine dehydropolymerization reactions to form growing polyborazylene nanotubes that then undergo thermal ceramic conversion to BNNTs. The reactions with decaborane require the additional step of a reaction with ammonia to generate the BNNTs. Decaborane is known to react with ammonia at high temperatures to form BN, and decaborane/ammonia CVD reactions have previously been used to form both thick and thin BN coatings on a variety of substrates.[99,112−114] BNNT formation from decaborane could thus be envisioned to occur by a process involving the initial binding of decaborane at the catalytically active sites, followed by its sequential conversion to BN and BNNTs upon reaction with ammonia. Alternately, the Lewis acidic decaborane could be reacting with ammonia in the gas phase to form decaborane-ammonia adducts,[97] which then further decompose into (BNH_x) fragments that bind to the catalyst sites to grow the BNNTs.

■ CONCLUSIONS

Both borazine and decaborane have been shown to be useful molecular precursors to BNNTs using the floating-catalyst CCVD method with each precursor having its own advantages. The amine-borane borazine is a single-source precursor containing both boron and nitrogen that forms primarily double-walled BNNTs. On the other hand, reactions with the

dx.doi.org/10.1021/cm3006088 | Chem. Mater. 2012, 24, 2872−2879

boron hydride decaborane primarily yield longer multiwall BNNTs, and while these reactions require the additional step of reaction with ammonia, the higher BNNT yields and the ease of handling and commercial availability of decaborane are distinct advantages. The only other boron hydride that has been previously used for BNNT synthesis is diborane, which is a toxic and highly explosive gas that will spontaneously ignite in air.[115] The increase in safety that can be achieved with the use of decaborane is clearly a significant improvement over diborane based syntheses. The CCVD method employing either of the borazine or decaborane molecular precursors is a potentially scalable route to BNNTs that offers the possibility to produce BNNT materials continuously in a manner similar to the HiPco or CoMoCAT processes[77,116] used in the large scale production of carbon nanotubes.

EXPERIMENTAL SECTION

Materials. Nickelocene was purchased from Strem Chemicals. Borazine was synthesized by the literature method.[117,118] Decaborane was freshly sublimed before use. Ultra high purity (UHP) grade nitrogen, ammonia, and hydrogen gases were purchased from Airgas.

Experimental Procedures. The CCVD experimental set up used for the syntheses of BNNTs from borazine is shown in the Supporting Information, Figure S1 and that used for the syntheses from decaborane is shown in Supporting Information, Figure S2. All manipulations were carried out using standard high vacuum or inert-atmosphere techniques as described by Shriver and Drezdzon.[119] All CCVD experiments were carried out at atmospheric pressure. The gas flow rates were controlled by mass flow controllers (MFC) with suitable flow ranges, calibrated in standard cm^3/min (sccm). The effective flow rate of precursors (F_{pr}) was estimated by the equation F_{pr} = (vapor pressure of precursor/760 Torr) × flow rate of carrier gas (**eq 1**), assuming the precursors were at equilibrium vapor pressures at the specified temperatures. The mole-fractions of precursors in the growth zone (χ_{pr}) were estimated by the equation $\chi_{pr} = F_{pr}/F_{total}$ (**eq 2**), where, F_{total} is the total of flow rates of all gases into the growth zone.

BNNTs Grown from Borazine. A flow-through vessel containing solid nickelocene (~100 mg) was heated with a heating tape at 80−90 °C. At the same time, a bubbler containing liquid borazine was maintained at the temperature of the desired borazine vapor pressure (~22−166 Torr, −20−20 °C) using an acetone/dry ice cooling bath. The flow rates given for exp. F, with a borazine pressure of ~22 Torr, correspond to 0.02 g/h of borazine (Table 1). The carrier gas for nickelocene was nitrogen (exp. H), hydrogen (exp. A) or ammonia (all other exps.), while nitrogen was the borazine carrier gas. Best results were obtained with ammonia as the carrier for nickelocene. The gas streams were allowed to combine as they flowed into the hot zone of the furnace. An additional flow of ammonia was supplied to the furnace through another inlet in exp. H. In separate experiments, the growth temperature was varied over 1000−1300 °C with the optimum temperature found at 1200 °C.

BNNTs Grown from Decaborane. A flow-through vessel containing solid nickelocene (~120 mg), was heated under ammonia (exp. P) or nitrogen (all other exps.) flow with a heating tape to the desired temperature (80−100 °C). At the same time, a separate flow-through vessel containing solid decaborane (~0.5 g) under a nitrogen flow was heated with a heating tape at the temperature (~10−20 Torr, 90−100 °C) of the desired decaborane vapor pressure. The flow rates given for exp. J (Table 2), with a decaborane pressure of ~20 Torr, correspond to 0.05 g/h of decaborane. The two gas streams were allowed to combine as they flowed into the hot zone of the furnace. Additional flows of ammonia and/or nitrogen were supplied to the furnace through other inlets. In separate experiments, the growth temperature was varied over 1100−1400 °C (exps. I, J, K, Q, R, Table 2).

Experiments at 1200−1300 °C (Tables 2 and 3) investigated the effects of the relative flow rates (F_{pr}) and mole-fractions (χ_{pr}) of the decaborane precursor, the nickelocene catalyst, the ammonia reactant, and the nitrogen carrier gas on the BNNT yield and quality. The precursor flow rates F_{pr} and the mole-fractions χ_{pr} were calculated using **eqs 1** and **2** and were controlled by either changing the precursor vapor pressure or carrier gas flow rate. The optimum conditions for the decaborane/ammonia reactions (Tables 2 and 3) proved to be growth at 1200 °C, with the decaborane heated at 90 °C (exp. J, ~10 Torr; 12 sccm nitrogen) or at 100 °C (exp. K, ~20 Torr; 5 sccm nitrogen), along with flows of nickelocene (~1.1 Torr; 100 sccm nitrogen) and ammonia (100 sccm) into the furnace for 3 h. Under these conditions, the decaborane to nickelocene mole ratios in the growth zone were nearly equal. When a lower ratio of decaborane to nickelocene was used, that is, $F_{deca} < F_{Ni}$ and $\chi_{deca} < \chi_{Ni}$, which was attained by lowering the decaborane pressure (F_{deca}/F_{Ni} ~1:2, exp. L) or by increasing either the nickelocene pressure (F_{deca}/F_{Ni} ~1:3, exp. O) or the nickelocene carrier gas flow rate (F_{deca}/F_{Ni} ~1:3, exp. N), then the BNNT yields decreased, with the BNNTs from exp. N being less than 100 nm long. In contrast to the results with borazine, when ammonia was the carrier for nickelocene (exp. P), a reduced BNNT yield was observed. In all experiments, the as-grown materials also contained BN-encapsulated Ni particles and flakes of turbostratic BN.[100] The BNNTs were also often coated with other BN nanostructures (Supporting Information, Figure S6). To try to minimize the formation of these other BN materials, nitrogen was introduced through a separate inlet to dilute the precursor concentrations in the reaction zone while maintaining the same flow rates (exp. M), but this led to greatly decreased BNNT yields.

Attempted NT Growth from Borazine or Decaborane without the Ni Catalyst. No BNNT growth was observed when (1) borazine (~22 Torr (−20 °C); 3 sccm nitrogen) was reacted with ammonia (100 sccm) for ~3 h at 1200 °C (control exp. I), or (2) decaborane (~10 Torr (90 °C); 12 sccm nitrogen), ammonia (100 sccm), and nitrogen (100 sccm) were reacted for ~1.5 h at 1200 °C (control exp. II).

Attempted NT Growth from Decaborane without Ammonia. No NT growth was observed when decaborane (~10 Torr (90 °C); 12 sccm nitrogen), nickelocene (80 °C; 100 sccm nitrogen), and nitrogen (100 sccm) were reacted for ~1.5 h at 1200 °C (control exp. III).

Sample Preparation for Analyses. During the course of the reactions, the BN nanomaterials were deposited at room temperature on a collection grid with a glass fiber filter near the downstream exit of the pyrolysis tube. The as-grown samples were washed off the collection grid with ethanol. The solution was ultrasonicated and then dropped on a holey carbon TEM grid to enable study by TEM and EELS. Samples for SEM analyses were prepared by depositing the BN nanomaterials on carbon tape on SEM stubs and sputter coating these materials with Au/Pd.

Oxidation Studies. A sample of the BNNTs synthesized from borazine at 1200 °C (exp. F, Table 1) was placed in a boron nitride boat inside the pyrolysis tube of the Lindberg furnace. The ends of the tube were left open to air, and the temperature was ramped to 600 °C. After being held at this temperature for 30 min, the furnace was cooled to room temperature, and the BNNTs removed for analysis by TEM and EELS (Supporting Information, Figure S5).

Physical Measurements. The TEM and EELS analyses at University of Pennsylvania employed a JEOL 2010F, while those at Purdue University used a FEI Titan 80-300 S/TEM. SEM images were taken with a FEI Strata DB235. Sputter coating was done by a Cressington Sputter Coater 108.

ASSOCIATED CONTENT

Supporting Information

Schematic diagrams of the CCVD apparatus used for BNNT growth from borazine and decaborane; figures showing TEM images of BNNTs produced under different conditions; electron energy loss spectrum (EELS) of BNNTs after air oxidation. This material is available free of charge via the Internet at http://pubs.acs.org.

AUTHOR INFORMATION

Corresponding Author

*E-mail: Benji.Maruyama@wpafb.af.mil (B.M.), lsneddon@sas.upenn.edu (L.G.S.).

Present Addresses

[⊥]Samsung Electro-Mechanics Co., Ltd., Suwon, Republic of Korea.

[⊗]Center for Functional Nanomaterials, Brookhaven National Laboratory, Upton, New York 11973, United States.

Notes

The authors declare no competing financial interest.

ACKNOWLEDGMENTS

The National Science Foundation and the Air Force Office of Scientific Research through the UTC contract (Collaborative Research and Development (CR&D F33615-03-D-5801)) are gratefully acknowledged for the support of this research.

REFERENCES

(1) Oberlin, A.; Endo, M.; Koyama, T. *J. Cryst. Growth* **1976**, *32*, 335−349.

(2) Iijima, S. *Nature* **1991**, *354*, 56−58.

(3) Dresselhaus, M. S.; Dresselhaus, G.; Avouris, P. *Carbon Nanotubes Synthesis, Structure, Properties and Applications*; Springer: New York, 2001.

(4) Chen, Y.; Zou, J.; Campbell, S. J.; Caer, G. L. *Appl. Phys. Lett.* **2004**, *84*, 2430−2432.

(5) Blase, X.; Rubio, A.; Louie, S. G.; Cohen, M. L. *Europhys. Lett.* **1994**, *28*, 335−340.

(6) Rubio, A.; Corkill, J. L.; Cohen, M. L. *Phys. Rev. B* **1994**, *49*, 5081−5084.

(7) Blase, X.; Rubio, A.; Louie, S. G.; Cohen, M. L. *Phys. Rev. B* **1995**, *51*, 6868−6875.

(8) Czerw, R.; Webster, S.; Carroll, D. L.; Vieira, S. M. C.; Birkett, P. R.; Rego, C. A.; Roth, S. *Appl. Phys. Lett.* **2003**, *83*, 1617−1619.

(9) Arenal, R.; Stephan, O.; Kociak, M.; Taverna, D.; Loiseau, A.; Colliex, C. *Phys. Rev. Lett.* **2005**, *95*, 127601/1−127601/4.

(10) Khoo, K. H.; Mazzoni, M. S. C.; Louie, S. G. *Phys. Rev. B* **2004**, *69*, 201401/1−201401/4.

(11) Ishigami, M.; Sau, J. D.; Aloni, S.; Cohen, M. L.; Zettl, A. *Phys. Rev. Lett.* **2005**, *94*, 056804/1−056804/4.

(12) Chopra, N. G.; Zettl, A. *Solid State Commun.* **1998**, *105*, 297−300.

(13) Chang, C. W.; Han, W.; Zettl, A. *Appl. Phys. Lett.* **2005**, *86*, 173102/1−173102/3.

(14) Tang, C.; Bando, Y.; Liu, C.; Fan, S.; Zhang, J.; Ding, X.; Golberg, D. *J. Phys. Chem. B* **2006**, *110*, 10354−10357.

(15) Chang, C. W.; Fennimore, A. M.; Afanasiev, A.; Okawa, D.; Ikuno, T.; Garcia, H.; Li, D.; Majumdar, A.; Zettl, A. *Phys. Rev. Lett.* **2006**, *97*, 085901/1−085901/4.

(16) Ma, R.; Golberg, D.; Bando, Y.; Sasaki, T. *Phil. Trans. R. Soc. Lond. A* **2004**, *362*, 2161−2186.

(17) Golberg, D.; Bando, Y.; Tang, C. C.; Zhi, C. *Adv. Mater.* **2007**, *19*, 2413−2432.

(18) Terrones, M.; Romo-Herrara, J. M.; Cruz-Silva, E.; Lopez-Urias, F.; Munoz-Sandoval, E.; Valezquez-Salazar, J. J.; Terrones, H.; Bando, Y.; Golberg, D. *Mater. Today* **2007**, *10*, 30−38.

(19) Golberg, D.; Bando, Y.; Huang, Y.; Terao, T.; Mitome, M.; Tang, C.; Zhi, C. *ACS Nano* **2010**, *4*, 2979−2993.

(20) Golberg, D.; Bando, Y.; Huang, Y.; Xu, Z.; Wei, X.; Bourgeois, L.; Wang, M.-S.; Zeng, H.; Lin, J.; Zhi, C. *Isr. J. Chem.* **2010**, *50*, 405−416.

(21) Hamilton, E. J. M.; Dolan, S. E.; Mann, C. M.; Colijn, H. O.; McDonald, C. A.; Shore, S. G. *Science* **1993**, *260*, 659−661.

(22) Loiseau, A.; Willaime, F.; Demoncy, N.; Hug, G.; Pascard, H. *Phys. Rev. Lett.* **1996**, *76*, 4737−4740.

(23) Chopra, N. G.; Luyken, R. J.; Cherrey, K.; Crespi, V. H.; Cohen, M. L.; Louie, S. G.; Zettl, A. *Science* **1995**, *269*, 966−967.

(24) Suenaga, K.; Colliex, C.; Demoncy, N.; Loiseau, A.; Pascard, H.; Willaime, F. *Science* **1997**, *278*, 653−655.

(25) Loiseau, A.; Willaime, F.; Demoncy, N.; Schramchenko, N.; Hug, G.; Colliex, C.; Pascard, H. *Carbon* **1998**, *36*, 743−752.

(26) Saito, Y.; Maida, M.; Matsumoto, T. *Jpn. J. Appl. Phys.* **1999**, *38*, 159−163.

(27) Altoe, M. V. P.; Sprunck, J. P.; Gabriel, J.-C. P.; Bradley, K. *J. Mater. Sci.* **2003**, *38*, 4805−4810.

(28) Narita, I.; Oku, T. *Diamond Relat. Mater.* **2003**, *12*, 1912−1917.

(29) Nishiwaki, A.; Oku, T. *J. Eur. Ceram. Soc.* **2006**, *26*, 435−441.

(30) Golberg, D.; Bando, Y.; Erements, M.; Takemura, K.; Kurashima, K.; Yusa, H. *Chem. Phys. Lett.* **1997**, *279*, 191−196.

(31) Lee, R. S.; Gavillet, J.; Lamy de la Chapelle, M.; Loiseau, A.; Cochon, J.-L.; Pigache, D.; Thibault, J.; Willaime, F. *Phys. Rev. B* **2001**, *64*, 121405/1−121405/4.

(32) Golberg, D.; Rode, A.; Bando, Y.; Mitome, M.; Gamaly, E.; Luther-Davies, B. *Diamond Relat. Mater.* **2003**, *12*, 1269−1274.

(33) Wang, J. S.; Kayastha, V. K.; Yap, Y. K.; Fan, Z.; Lu, J. G.; Pan, Z.; Ivanov, I. N.; Puretzky, A. A.; Geohegan, D. B. *Nano Lett.* **2005**, *5*, 2528−2532.

(34) Arenal, R.; Stephan, O.; Cochon, J.; Loiseau, A. *J. Am. Chem. Soc.* **2007**, *129*, 16183−16189.

(35) Xie, M.; Wang, J.; Yap, Y. K. *J. Phys. Chem. C* **2010**, *114*, 16236−16241.

(36) Chen, Y.; Chadderton, L. T.; Fitzgerald, J.; Williams, J. S. *Appl. Phys. Lett.* **1999**, *74*, 2960−2962.

(37) Chen, Y.; Fitzgerald, J.; Williams, J. S.; Bulcock, S. *Chem. Phys. Lett.* **1999**, *299*, 260−264.

(38) Chen, Y.; Fitzgerald, J.; Williams, J. S.; Willis, P. *J. Metastable Nanocryst. Mater.* **1999**, *2*−*6*, 173−178.

(39) Yu, J.; Chen, Y.; Wuhrer, R.; Liu, Z.; Ringer, S. P. *Chem. Mater.* **2005**, *17*, 5172−5176.

(40) Bae, S. Y.; Seo, H. W.; Park, J.; Choi, Y. S.; Park, J. C.; Lee, S. Y. *Chem. Phys. Lett.* **2003**, *374*, 534−541.

(41) Chen, X.; Gao, X. P.; Zhang, H.; Zhou, Z.; Hu, W. K.; Pan, G. L.; Zhu, H. Y.; Yan, T. Y.; Song, D. Y. *J. Phys. Chem. B* **2005**, *109*, 11525−11529.

(42) Tang, C. C.; Lamy de la Chapelle, M.; Li, P.; Liu, Y. M.; Dang, H. Y.; Fan, S. S. *Chem. Phys. Lett.* **2001**, *342*, 492−496.

(43) Tang, C. C.; Ding, X. X.; Huang, X. T.; Gan, Z. W.; Qi, S. R.; Liu, W.; Fan, S. S. *Chem. Phys. Lett.* **2002**, *356*, 254−258.

(44) Nishiwaki, A.; Oku, T.; Tokoro, H.; Fujii, S. *Diamond Relat. Mater.* **2005**, *14*, 1163−1168.

(45) Tang, C. C.; Bando, Y.; Sato, T. *Appl. Phys. A: Mater. Sci. Process.* **2002**, *75*, 681−685.

(46) Tang, C.; Bando, Y.; Golberg, D. *J. Solid State Chem.* **2004**, *177*, 2670−2674.

(47) Tang, C.; Bando, Y.; Sato, T.; Kurashima, K. *Chem. Commun.* **2002**, 1290−1291.

(48) Zhi, C.; Bando, Y.; Tan, C.; Golberg, D. *Solid State Commun.* **2005**, *135*, 67−70.

(49) Lee, C. H.; Wang, J.; Kayastha, V. K.; Huang, J. Y.; Yap, Y. K. *Nanotechnology* **2008**, *19*, 455605/1−455605/5.

(50) Lee, C. H.; Xie, M.; Kayastha, V.; Wang, J.; Yap, Y. K. *Chem. Mater.* **2010**, *22*, 1782−1787.

(51) Huang, Y.; Lin, J.; Tang, C.; Bando, Y.; Zhi, C.; Zhai, T.; Dierre, B.; Sekiguchi, T.; Golberg, D. *Nanotechnology* **2011**, *22*, 145602/1−145602/9.

(52) Fu, J. J.; Lu, Y. N.; Xu, H.; Huo, K. F.; Wang, X. Z.; Li, L.; Hu, Z.; Chen, Y. *Nanotechnology* **2004**, *15*, 727−730.

(53) Tang, C.; Bando, Y.; Sato, T. *Chem. Phys. Lett.* **2002**, *362*, 185−189.

(54) Smith, M. W.; Jordan, K. C.; Park, C.; Kim, J.-W.; Lillehei, P. T.; Crooks, R.; Harrison, J. S. *Nanotechnology* **2009**, *20*, 505604/1−505604/6.

(55) Ma, R.; Bando, Y.; Sato, T. *Chem. Phys. Lett.* **2001**, *337*, 61−64.

(56) Ma, R.; Bando, Y.; Sato, T.; Kurashima, K. *Chem. Mater.* **2001**, *13*, 2965−2971.
(57) Fan, Y.; Wang, Y.; Lou, J.; Xu, S.; Zhang, L.; An, L. *J. Am. Ceram. Soc.* **2006**, *89*, 740−742.
(58) Zhong, B.; Huang, X.; Wen, G.; Yu, H.; Zhang, X.; Zhang, T.; Bai, H. *Nanoscale Res. Lett.* **2011**, *6*, 36.
(59) Li, J.; Zhang, L.; Gu, Y.; Qian, Q.; Wang, J.; Zhao, G.; Pan, X. *Chem. Lett.* **2011**, *40*, 540−541.
(60) Wang, J.; Zhang, L.; Zhao, G.; Gu, Y.; Zhang, Z.; Zhang, F.; Wang, W. *J. Solid State Chem.* **2011**, *184*, 2478−2484.
(61) Zhang, L.; Wang, J.; Gu, Y.; Zhao, G.; Qian, Q.; Li, J.; Pan, X.; Zhang, Z. *Mater. Lett.* **2012**, *67*, 17−20.
(62) Bechelany, M.; Brioude, A.; Bernard, S.; Stadelmann, P.; Cornu, D.; Miele, P. *CrystEngComm.* **2011**, *13*, 6526−6530.
(63) Lourie, O. R.; Jones, C. R.; Bartlett, M.; Gibbons, P. C.; Ruoff, R. S.; Buhro, W. E. *Chem. Mater.* **2000**, *12*, 1808−1810.
(64) Guo, L.; Singh, R. N. *Nanotechnology* **2008**, *19*, 065601/1−065601/6.
(65) Guo, L.; Singh, R. N. *Phys. E* **2009**, *41*, 448−453.
(66) Su, C.-Y.; Juang, Z.-Y.; Chen, K.-F.; Cheng, B.-M.; Chen, F.-R.; Leou, K.-C.; Tsai, C.-H. *J. Phys. Chem. C* **2009**, *113*, 14681−14688.
(67) Su, C.-Y.; Chu, W.-Y.; Juang, Z.-Y.; Chen, K.-F.; Cheng, B.-M.; Chen, F.-R.; Leou, K.-C.; Tsai, C.-H. *J. Phys. Chem. C* **2009**, *113*, 14732−14738.
(68) Kim, M. J.; Chatterjee, S.; Kim, S. M.; Stach, E. A.; Bradley, M. G.; Pender, M. J.; Sneddon, L. G.; Maruyama, B. *Nano Lett.* **2008**, *8*, 3298−3302.
(69) Sen, R.; Govindaraj, A.; Rao, C. N. R. *Chem. Mater.* **1997**, *9*, 2078−2081.
(70) Sen, R.; Govindaraj, A.; Rao, C. N. R. *Chem. Phys. Lett.* **1997**, *267*, 276−280.
(71) Satishkumar, B. C.; Govindaraj, A.; Sen, R.; Rao, C. N. R. *Chem. Phys. Lett.* **1998**, *293*, 47−52.
(72) Cheng, H. M.; Li, F.; Su, G.; Pan, H. Y.; He, L. L.; Sun, X.; Dresselhaus, M. S. *Appl. Phys. Lett.* **1998**, *72*, 3282−3284.
(73) Satishkumar, B. C.; Govindaraj, A.; Rao, C. N. R. *Chem. Phys. Lett.* **1999**, *307*, 158−162.
(74) Nikolaev, P.; Bronikowski, M. J.; Bradley, R. K.; Rohmund, F.; Colbert, D. T.; Smith, K. A.; Smalley, R. E. *Chem. Phys. Lett.* **1999**, *313*, 91−97.
(75) Satishkumar, B. C.; Thomas, P. J.; Govindaraj, A.; Rao, C. N. R. *Appl. Phys. Lett.* **2000**, *77*, 2530−2532.
(76) Deepak, F. L.; Govindaraj, A.; Rao, C. N. R. *Chem. Phys. Lett.* **2001**, *345*, 5−10.
(77) Bronikowski, M. J.; Willis, P. A.; Colbert, D. T.; Smith, K. A.; Smalley, R. E. *J. Vac. Sci. Technol. A* **2001**, *19*, 1800−1805.
(78) Govindaraj, A.; Rao, C. N. R. *Pure Appl. Chem.* **2002**, *74*, 1571−1580.
(79) Govindaraj, A.; Rao, C. N. R. *Acc. Chem. Res.* **2002**, *35*, 998−1007.
(80) Wagner, R. S.; Ellis, W. C. *Appl. Phys. Lett.* **1964**, *4*, 89−90.
(81) Tibbetts, G. G. *J. Cryst. Growth* **1984**, *66*, 632−638.
(82) Schmidt, V.; Gösele, U. *Science* **2007**, *316*, 698−699.
(83) Nessim, G. D. *Nanoscale* **2010**, *2*, 1306−1323.
(84) Kubota, Y.; Watanabe, K.; Tsuda, O.; Taniguchi, T. *Science* **2007**, *317*, 932−934.
(85) Turnbull, A. G. *Aust. J. Chem.* **1967**, *20*, 2059−2067.
(86) Turnbull, A. G. *Aust. J. Chem.* **1967**, *20*, 2757−2760.
(87) *Gmelin Handbuch der Anorganishen Chemie, Borazine and Its Derivatives*; Springer-Verlag: New York, 1978; Vol. *17*.
(88) Gaines, D. F.; Borlin, J. In *Boron Hydride Chemistry*; Muetterties, E. L., Ed.; Academic Press: New York, 1975; Chapter 7 and references therein.
(89) Paffett, M. T.; Simonson, R. J.; Papin, P.; Paine, R. T. *Surf. Sci.* **1990**, *232*, 286−296.
(90) Nagashima, A.; Tejima, N.; Gamou, Y.; Kawai, T.; Oshima, C. *Phys. Rev. Lett.* **1995**, *75*, 3918−3921.
(91) Grad, G. B.; Blaha, P.; Schwarz, K.; Auwarter, W.; Greber, T. *Phys. Rev. B* **2003**, *68*, 085404.
(92) Auwarter, W.; Suter, H. U.; Sachdev, H.; Greber, T. *Chem. Mater.* **2004**, *16*, 343−345.
(93) Preobrajenski, A. B.; Vinogradov, A. S.; Martensson, N. *Surf. Sci.* **2005**, *582*, 21−30.
(94) Orlando, F.; Lacriprete, R.; Lacovig, P.; Boscarato, I.; Baraldi, I.; Lizzit, S. *J. Phys. Chem. C* **2012**, *116*, 157−164 , and references therein.
(95) Fazen, P. J.; Beck, J. S.; Lynch, A. T.; Remsen, E. E.; Sneddon, L. G. *Chem. Mater.* **1990**, *2*, 96−97.
(96) Fazen, P. J.; Remsen, E. E.; Beck, J. S.; Carroll, P. J.; McGhie, A. R.; Sneddon, L. G. *Chem. Mater.* **1995**, *7*, 1942−1956.
(97) *Gmelin Handbuch der Anorganischen Chemie, Boron-Hydrogen Compounds*; Springer-Verlag: New York, 1979;Vol. *20*, Part 3.
(98) Perel, A. S.; Loizides, W. K.; Reynolds, W. E. *Rev. Sci. Instrum.* **2002**, *73*, 877−879.
(99) Chatterjee, S.; Luo, Z.; Acerce, M.; Yates, D. M.; Johnson, A. T. C.; Sneddon, L. G. *Chem. Mater.* **2011**, *23*, 4414−4416.
(100) Paine, R. T.; Narula, C. K. *Chem. Rev.* **1990**, *90*, 73−91.
(101) Menon, M.; Srivastava, D. *Chem. Phys. Lett.* **1999**, *307*, 407−412.
(102) Saito, Y.; Maida, M. *J. Phys. Chem. A* **1999**, *103*, 1291−1293.
(103) Golberg, D.; Bando, Y.; Stephan, O.; Kurashima, K. *Appl. Phys. Lett.* **1998**, *73*, 2441−2443.
(104) Han, W.; Bando, Y.; Kurashima, K.; Sato, T. *Jpn. J. Appl. Phys.* **1999**, *38*, L755−L757.
(105) Oku, T.; Hirano, T.; Kuno, M.; Kusunose, T.; Niihara, K.; Suganama, K. *Mater. Sci. Eng.* **2000**, *B74*, 206−217.
(106) Wang, X.; Xie, Y.; Guo, Q. *Chem. Commun.* **2003**, 2688−2689.
(107) Xu, F.; Xie, Y.; Zhang, X.; Zhang, S.; Liu, X.; Tian, X. *Inorg. Chem.* **2004**, *43*, 822−829.
(108) Ahn, C. C.; Krivanek, O. L. *EELS Atlas*; Gatan Inc.: Warrendale, PA, 1983.
(109) Arenal, R.; Stephan, O.; Loiseau, A.; Colliex, C. *Microsc. Microanal.* **2007**, *13* (Suppl. 2), 1240(CD)−1241CD.
(110) Su, K.; Sneddon, L. G. *Chem. Mater.* **1993**, *5*, 1659−1668.
(111) Kher, S. S.; Spencer, J. T. *Chem. Mater.* **1992**, *4*, 538−544.
(112) Nakamura, K. *J. Electrochem. Soc.* **1985**, *132*, 1757−1762.
(113) Kim, Y. G.; Dowben, P. A.; Spencer, J. T.; Ramseyer, G. O. *J. Vac. Sci. Technol. A* **1989**, *7*, 2796−2799.
(114) Zhang, Z.; Kim, Y.-G.; Dowben, P. A.; Spencer, J. T. *Mater. Res. Soc. Symp. Proc.* **1989**, *131*, 407−412.
(115) Long, L. H. In *Progress in Inorganic Chemistry*; Lippard, S. J., Ed.; Wiley-Interscience Publishers: New York, 1972; Vol. *15*; Chapter 1 and references therein.
(116) Kitiyanan, B.; Alvarez, W. E.; Harwell, J. H.; Resasco, D. E. *Chem. Phys. Lett.* **2000**, *317*, 497−503.
(117) Wideman, T.; Sneddon, L. G. *Inorg. Chem.* **1995**, *34*, 1002−1003.
(118) Wideman, T.; Fazen, P. J.; Lynch, A. T.; Su, K.; Remsen, E. E.; Sneddon, L. G. *Inorg. Synth.* **1998**, *32*, 232−242.
(119) Shriver, D. F.; Drezdzon, M. A. *Manipulation of Air-Sensitive Compounds*, 2nd ed.; Wiley: New York, 1986.